AIP | Journal of Applied Physics

Electronic and elastic properties of yttrium gallium garnet under pressure from ab initio studies

V. Monteseguro, P. Rodríguez-Hernández, V. Lavín, F. J. Manjón, and A. Muñoz

Citation: J. Appl. Phys. **113**, 183505 (2013); doi: 10.1063/1.4804133
View online: http://dx.doi.org/10.1063/1.4804133
View Table of Contents: http://jap.aip.org/resource/1/JAPIAU/v113/i18
Published by the American Institute of Physics.

Additional information on J. Appl. Phys.

Journal Homepage: http://jap.aip.org/
Journal Information: http://jap.aip.org/about/about_the_journal
Top downloads: http://jap.aip.org/features/most_downloaded
Information for Authors: http://jap.aip.org/authors

ADVERTISEMENT

Downloaded 09 May 2013 to 158.42.242.92. This article is copyrighted as indicated in the abstract. Reuse of AIP content is subject to the terms at: http://jap.aip.org/about/rights_and_permissions

JOURNAL OF APPLIED PHYSICS **113**, 183505 (2013)

Electronic and elastic properties of yttrium gallium garnet under pressure from *ab initio* studies

V. Monteseguro,[1,2] P. Rodríguez-Hernández,[2] V. Lavín,[1] F. J. Manjón,[3] and A. Muñoz[2,a)]
[1]*Departamento de Física Fundamental y Experimental, Electrónica y Sistemas, and MALTA Consolider Team, Universidad de La Laguna, 38200 San Cristóbal de La Laguna, Santa Cruz de Tenerife, Spain*
[2]*Departamento de Física Fundamental II, Instituto de Materiales y Nanotecnología, Universidad de La Laguna and MALTA Consolider Team, La Laguna 38205, Tenerife, Spain*
[3]*Instituto de Diseño para la Fabricación y Producción Automatizada, and MALTA Consolider Team, Universitat Politècnica de València, 46022 Valencia, Spain*

(Received 18 February 2013; accepted 22 April 2013; published online 9 May 2013)

In this paper, we present an *ab initio* study within the framework of density functional theory employing the generalized gradient approximation applied to the study of the structural, elastic, and electronic properties of yttrium gallium garnet, $Y_3Ga_5O_{12}$, under hydrostatic pressure. The calculated structural ground state properties are in good agreement with the available experimental data. Pressure dependence of the elastic constants and the mechanical stability are analysed up to 90 GPa, showing that the garnet is mechanically unstable above 84 GPa. We also present the electronic band structure calculations which show that upon compression the fundamental direct gap first increases up to 63 GPa and later monotonically decreases under pressure. © *2013 AIP Publishing LLC*.
[http://dx.doi.org/10.1063/1.4804133]

I. INTRODUCTION

Nowadays, oxide garnets are being used for technological application in the field of optical materials, solar energy, and optical imaging as well as active elements for solid-state laser.[1,2] This is because their high thermal conductivity, hardness, and chemical and mechanical stability make them good host matrices for rare ions with interesting luminescence properties.

In the last decade, large efforts have been devoted to investigate the luminescence properties of RE^{3+}-doped nanostructured garnets, especially in the development of lasers and phosphors for lightning applications, 3-D optical imaging for displays, and as an alternative to quantum dots in the development of photonic and optoelectronic devices. The $Y_3Al_5O_{12}$ (YAG)[3,4] and the $Gd_3Ga_5O_{12}$(GGG)[5,6] nanostructures have proved to be efficient, flexible, and robust luminescent materials which can support high concentrations of RE^{3+} ions through substitution of Y^{3+} or Gd^{3+} ions without charge compensation. $Y_3Ga_5O_{12}$ (YGG) is also a good host matrix for rare earths; thus, it is worth researching its structural and electronic properties under high pressure which can provide important information about how a change in the RE^{3+} environment would affect its luminescence properties.

Oxide garnets have the general formula $A_3B_2C_3O_{12}$, where A denotes the dodecahedral, B the octahedral, and C the tetrahedral sites.[7] Garnets usually crystallize in the body centered cubic (bcc) structure (space group Ia3d). The cubic unit cell contains eight formula units (160 atoms) which are reduced to four formula units (80 atoms) in the primitive cell. In the bcc structure, the different A, B, and C cations have different coordinations: Y ions (A atoms) occupy 24 *c* sites and are coordinated with eight O atoms; Ga_{oct} ions (B atoms) occupy 16 *a* sites, with octahedral point symmetry (C_{3i}), and are coordinated with six O atoms; and Ga_{tet} ions (C atoms) occupy *24d* sites, with tetrahedral point symmetry (S_4), and are coordinated with four O atoms (Fig. 1). Finally, O atoms are located at 96*h* sites, defined by x, y, and z parameters. The high degree of complexity and the big amount of atoms in the garnet structure justify the absence of previous *ab initio* studies of the electronic, structural, and dynamical properties both at room and high pressures in many garnets and in particular in YGG. Most of the theoretical studies of some of most known garnets, like YAG, have been investigated by means of atomistic approach involving semi-empirical interatomic potentials with the rigid ion model (RIM),[8] and also few first-principles density functional theory (DFT) calculations for the ground-state have been performed.[7]

The use of *ab initio* DFT simulations for the study of materials under extreme conditions is a very well established technique in the field of high pressure semiconductor physics.[9] Therefore, since the high pressure properties of YGG garnet are essential for the quantitative understanding of its variety of properties, in this work, we report an extensive study of structural, electronic, and elastic properties of $Y_3Ga_5O_{12}$ garnet at ambient conditions and under hydrostatic pressure using state of the art first principles total-energy calculations. To our knowledge, there are not reported high pressures *ab initio* studies on the electronic and elastic properties of YGG. In this work, we provide valuable information that we hope will stimulate further the experimental study of this garnet under pressure. This paper is organized as follows. Details of first principles model calculation are presented in Sec. II, structural, elastic and electronic properties at ambient conditions and at high pressure are reported in Sec. III.

[a)]Author to whom correspondence should be addressed. Electronic mail: amunoz@marengo.dfis.ull.es.

 © 2013 AIP Publishing LLC

Downloaded 09 May 2013 to 158.42.242.92. This article is copyrighted as indicated in the abstract. Reuse of AIP content is subject to the terms at: http://jap.aip.org/about/rights_and_permissions

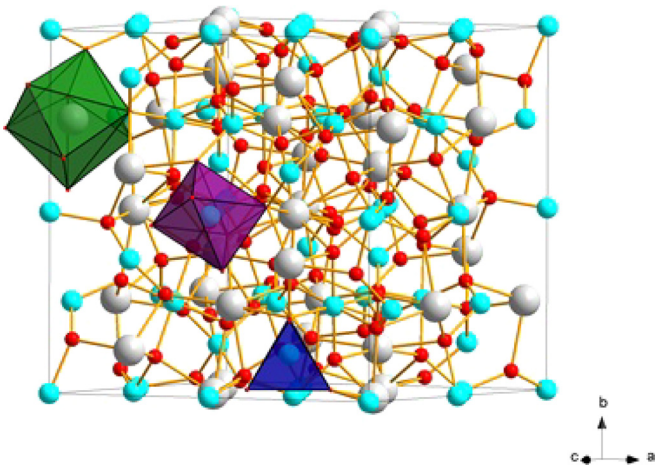

FIG. 1. The conventional unit cell with the polyhedra YO_8 (green), GaO_4 (violet), and GaO_6 (blue).

II. OVERVIEW OF THE CALCULATIONS

We have performed *ab initio* total-energy calculations at zero temperature within the density functional theory (DFT)[10] using the plane-wave method and the pseudopotential theory with the Vienna *ab initio* simulation package (VASP).[11] We have utilized ultra-soft pseudopotentials and the projector-augmented wave scheme (PAW)[12] implemented in this package to take into account the full nodal character of the all-electron charge density in the core region (for the Y atoms, 11 valence electrons are used ($4s^2 4p^6 5s^2 4d^1$), whereas for Ga atoms 13 valence electrons ($3d^{10} 4s^2 4p^1$) and for O atoms 6 valence electrons ($2s^2 2p^4$) are used). Basis set including plane waves up to an energy cutoff of 520 eV were employed in order to achieve highly converged results and accurate description of the electronic properties. The description of the exchange-correlation energy was performed with the generalized gradient approximation (GGA) with the PBEsol prescription.[13] A dense special k-points sampling for the Brillouin Zone (BZ) integration was performed in order to obtain very well converged energies and forces. At each selected volume, the structures were fully relaxed to their equilibrium configuration through the calculation of the forces and the stress tensor. It is useful to note that theoretical pressure, P(V), can be obtained within the DFT formalism as the same time as the total energy, E(V), but independently: P (like other derivatives of the energy) can be obtained from the calculated stress.[9] In the relaxed configurations, the forces on the atoms are less than 0.006 eV/Å and the deviation of the stress tensor from a diagonal hydrostatic form is less than 0.1 GPa. The calculated total energies versus volumes can be fitted using a standard equation of state, EOS, to determine the bulk modulus and its pressure derivatives.

Mechanical stability of homogeneous crystals is an interesting subject that can provide important information concerning the study of the structural transformations via the stability criteria. The elastic constants can be obtained computing the macroscopic stress for a small strain by using the stress theorem.[14] Alternatively, elastic constants can be also calculated using density functional perturbation theory (DFPT).[15] In this context, we have used the last method to calculate the ground state and fully relaxed structures at different pressures which were strained in different directions according to their symmetry. The total-energy variations were evaluated according to a Taylor expansion[16] for the total energy with respect to the applied strain, due to this fact it is important to check that the strain used in the calculations guarantees the harmonic behavior. This allows us to obtain the C_{ij} elastic constants in the Voigt notation and the number of independent elastic constant is reduced completely by crystalline symmetry.[17] The elastic constants allow the study of the mechanical properties and the mechanical stability of materials in the region where the strain-stress relations are still linear. Here, we are dealing with a cubic crystal, and for cubic symmetry there are only three independent elastic constants, C_{11}, C_{12}, and C_{44}, at zero pressure the Born stability criteria[18] for a cubic system are: $C_{11} + 2C_{12} > 0$, $C_{11} - C_{12} > 0$ and $C_{44} > 0$. Under hydrostatic pressure, the generalized Born mechanical stability criteria at any applied stress are:[19] $M_1 = c_{11} + 2c_{12} > 0$, $M_2 = c_{11} - c_{12} > 0$ and $M_3 = c_{44} > 0$, where the relevant elastic stiffness coefficients at the applied stress are $c_{11} = C_{11} - P$, $c_{12} = C_{12} + P$ and $c_{44} = C_{44} - P$. The system is mechanically stable when all the Born stability criteria are simultaneously satisfied. The elastic constants also enable to obtain the bulk modulus, B, which is the inverse of the compressibility and it is related with the resistance of the material to a uniform hydrostatic pressure. Additionally, we can obtain the isotropic shear modulus, G, the elastic moduli, E, the Poisson's ratio, ν, and the Zener anisotropy ratio, A. The above parameters describe the major elastic properties of a material and for a cubic crystal are given by

- $B = \dfrac{C_{11} + 2C_{12}}{3}$,
- $G = \dfrac{1}{2}\left[\dfrac{C_{11} - C_{12} + 3\ C_{44}}{5} + \dfrac{5\ C_{44}\ (C_{11} - C_{12})}{4\ C_{44} + 3(C_{11} - C_{12})}\right]$,
- $E = \dfrac{9\ B\ G}{(3B) + G}$,
- $\nu = \dfrac{E - 2G}{2G}$,
- $A = \dfrac{2C_{44}}{C_{11} - C_{12}}$. (1)

III. RESULTS AND DISCUSSION

A. Crystal structure and bulk properties

In this section, we are going to compare the experimental data already reported with the results obtained from our total-energy calculations. Fig. 2 shows the calculated energy-volume curve of the YGG garnet. At each selected volume, the structures were fully relaxed, our calculations, as mentioned, provide the pressure for a particular volume. The volume at equilibrium, the zero pressure volume, is the one with the lower energy, the forces nearly zero, and the stress tensor diagonal, and equal to zero. At zero pressure,

Downloaded 09 May 2013 to 158.42.242.92. This article is copyrighted as indicated in the abstract. Reuse of AIP content is subject to the terms at: http://jap.aip.org/about/rights_and_permissions

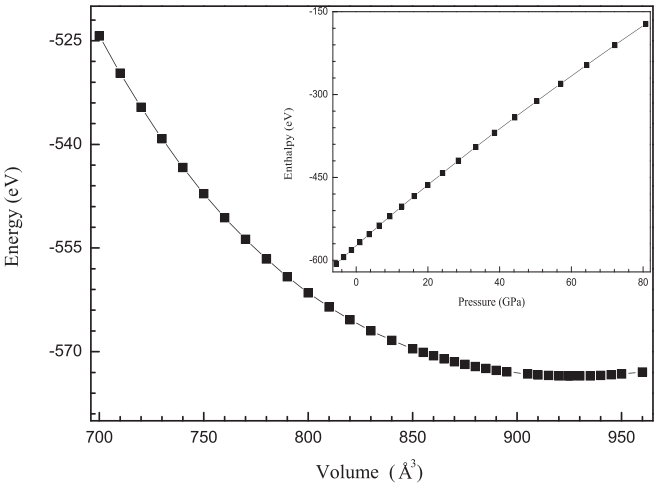

FIG. 2. Calculated total energy versus volume per primitive cell in YGG garnet. Inset shows the pressure dependence of enthalpy.

we obtain for the lattice constant and the volume of the primitive cell, 12.278 Å and 925.50 Å,[3] respectively (see Table I), with O atoms located at $x = -0.27739$, $y = 0.40000$, and $z = 0.19408$. These values are in good agreement with the available experimental data,[20] which differ less than 1% and 1.2%, respectively. The energy-volume data have been analyzed using a third-order Birch-Murnaghan equation of state, EOS.[21] The obtained volume at ambient pressure, V_0, corresponds to 926.7 Å^3 (this value is very similar to the theoretical zero pressure value), and the bulk modulus, B_0, and its pressure derivative, B_0', are summarized in Table I. This bulk modulus (170.7 GPa) is similar to those of most silicate garnets (between 150 and 180 GPa).[22] The YGG garnet has a smaller bulk modulus and bigger volume than other garnets such as the $Lu_3Ga_5O_{12}$ with volume 888.3 Å^3 and bulk modulus 181.2 GPa (Ref. 23) and the YAG with volume 867.9 Å^3 and bulk modulus 183.9 GPa.[7,24] Moreover, the bulk modulus of the YGG is lower than that of simple oxides as Y_2O_3 (bixbyite cubic phase) and Ga_2O_3 (monoclinic phase β) with bulk moduli of 212 GPa (Ref. 25) and between 174 and 202 GPa,[26] respectively.

The garnet structure can be viewed as interconnected polyhedra with shared O ions at the corners. As already commented, Y ions are dodecahedrally coordinated, Ga(16 a) ions are octahedrally coordinated, and Ga(24 d) ions are tetrahedrally coordinated[27] (Fig. 1). In particular, at ambient pressure, the YO_8 dodecahedron is slightly distorted with Y-O distances ranging from 2.34 to 2.42 Å. On the other hand, Ga_{oct}-O distances and Ga_{tet}-O distances are 1.84 Å and 1.99 Å, respectively (see Table II).

TABLE I. Lattice constant, volume, and bulk properties at 0 GPa of YGG.

	$Y_3Ga_5O_{12}$	
	Calculated (this work)	Experimental (Ref. 7)
Lattice constant (Å)	12.278	12.273
Volume (Å^3)	925.5	924.32
Bulk modulus (GPa), B	170.7	
Pressure coefficient, B′	4.46	

TABLE II. Nearest-neighbor distances between atoms at different pressures.

	Coordination distances (Å)		
	O GPa	43 GPa	75 GPa
Y-O	(2.34 to 2.42)	(2.24 to 2.32)	(2.16 to 2.21)
Ga_{tet}-O	1.84	1.87	1.72
Ga_{oct}-O	1.99	1.89	1.84
Y-Ga_{tet}	3.07	2.9	2.82

In a previous work on RE^{3+}-doped YAG, Papagelis *et al.* mentioned that in the garnet series only RE^{3+}-O distances, and consequently Y-O distances, vary significantly when the crystal volume decreases.[28] Figure 3 shows the theoretical pressure dependence of different interatomic distances in YGG. In YGG, all distances decrease with increasing pressure, but the Y-Ga_{tet} distance and the Y-O distances, in particular, the distance indicated by Y-O2 (see Fig. 3), vary more quickly. Therefore, our calculations confirm the finding of Papagelis *et al.*[28] Furthermore, since the Y-Ga_{tet} distance decreases, there is a greater influence between the dodecahedra and tetrahedra as pressure increases. The coordination distance between Y atoms and Ga_{tet} atoms decrease from 3.1 Å (0 GPa) to 2.8 Å (75 GPa) (Table II). It is also interesting to note that our calculations show that YO_8 dodecahedra are quite irregular at low pressures and continue to be irregular at high pressures.

B. Elastic properties

The whole set of elastic constants (see Table III) calculated fulfil the Born stability criteria for a cubic crystal

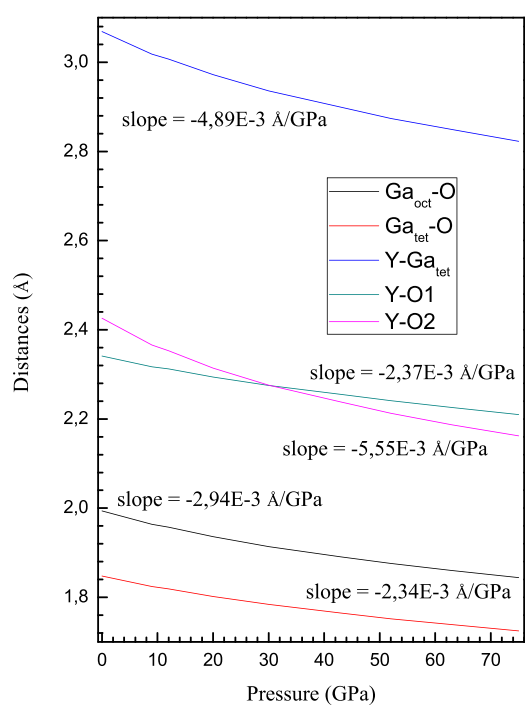

FIG. 3. The evolution of the distances between the following atoms, Y-O, Ga_{tet}-O, Ga_{oct}-O, and Y-Ga_{tet} with the pressure.

Downloaded 09 May 2013 to 158.42.242.92. This article is copyrighted as indicated in the abstract. Reuse of AIP content is subject to the terms at: http://jap.aip.org/about/rights_and_permissions

TABLE III. Generalized elastic constants, bulk modulus, isotropic shear modulus, Young's modulus, Poisson's ratio, Zener anisotropy ratio, and B/G ratio at ambient conditions.

Pressure 0 GPa								
C_{11} (GPa)	C_{12} (GPa)	C_{44} (GPa)	B (GPa)	G (GPa)	E (GPa)	ν	A	B/G
280.6	117.8	91.4	172.1	87.2	223.8	0.28	1.12	1.97

pointing the mechanical stability of the YGG at equilibrium pressure. It is also worth to know that the bulk modulus computed from the values of the elastic constants according to Eq. (1) is 172 GPa, which is in good agreement with the one obtained from the total-energy calculations of the volume using the fit with the Birch-Murnaghan EOS. Figure 4 shows the pressure dependence of the elastic stiffness coefficients of YGG. The generalized Born stability criteria, M_1, M_2, and M_3 versus pressure are plotted in Fig. 5. As observed, M_2 and M_3 stability criteria are violated in the present case at around 84 and 88 GPa, respectively; i.e., the tetragonal shear modulus $(C_{11}–C_{12}–P)/2$, and the shear modulus, C_{44}–P, are negative at these pressures. This result suggests that YGG becomes mechanically unstable above 84 GPa. The softening of C_{44} suggests shear instability of the cubic structure. In some cubic binary compounds, the C_{44} softening can be related with a phase transition mechanism.[29] Recent studies in YAG from empirical lattice dynamic calculations[8] and from atomistic model[30] report that YAG becomes mechanically unstable around 108 GPa due to the violation of the Born stability criteria by C_{44}. Reported experimental energy dispersive X-ray diffraction results suggest that the long-range crystalline order of Sm-doped YAG[31] is lost beyond 100 GPa. For gallium oxide garnets, Hua *et al.* have reported high pressure and high temperature studies of the Cr^{3+}, Nd^{3+}-doped GGG and the Cr^{3+}, Nd^{3+}-doped gadolinium scandium gallium garnet (GSGG).[32] The reported experimental results show that an amorphous phase appear over 76 and 84 GPa in GSGG and GGG, respectively. This result compares to aluminium garnets, like YAG garnet, which is

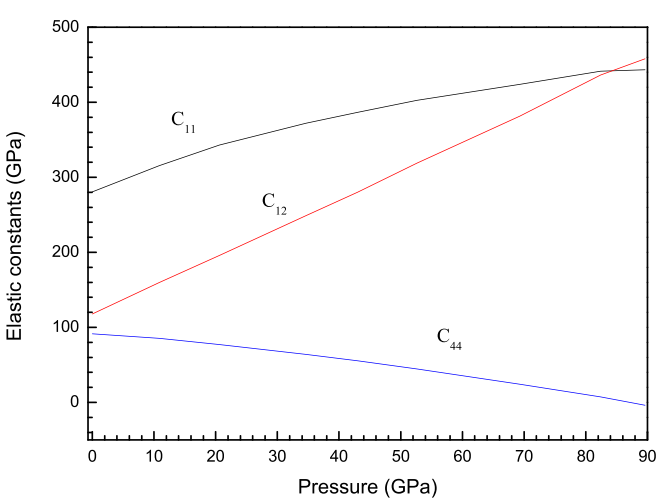

FIG. 4. Pressure evolution of the elastic stiffness coefficients from 0 to 116 GPa. The blue, red, and black lines correspond to C_{44}, C_{12}, and C_{11}, respectively.

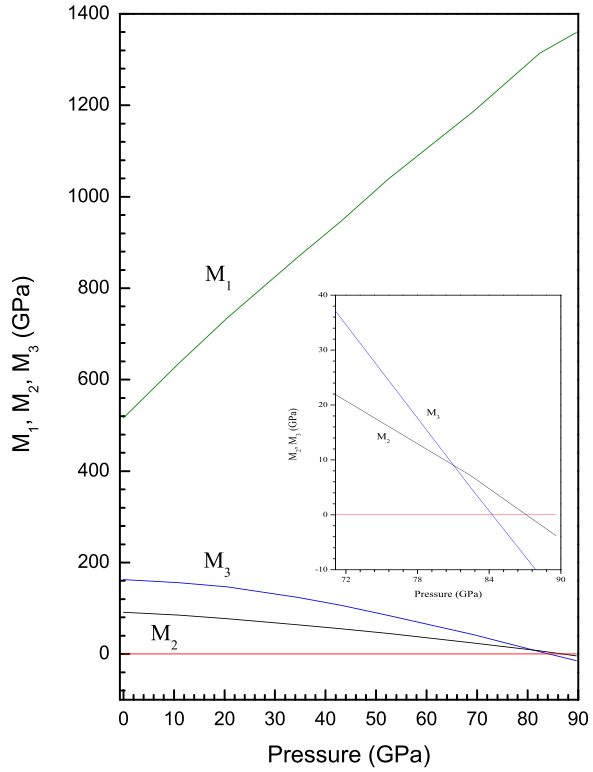

FIG. 5. Pressure evolution of the generalized Born stability criteria from 0 to 116 GPa.

found to retain its crystalline cubic phase up to 101 ± 4 GPa. Therefore, our results for YGG garnet are in good agreement with the reported experimental data for other gallium oxide garnets[32] and show that over 84 GPa, the generalized stability Born criteria are violated, thus suggesting that YGG will become amorphous around this pressure. In order to discuss the elastic properties of YGG at ambient pressure in detail, we summarize the values of the elastic moduli obtained from Eq. (1) in Table III. It is interesting to mention that we have obtained B/G = 1.97. Since the critical B/G value for ductile and brittle materials is 1.75, our B/G result suggests that YGG is a ductile material. The Zener anisotropy ratio is 1.12. Since this value is close to 1, it suggests that this compounds is an isotropic crystalline structure with a consistent big region of stability under compression. Finally, the other two important parameters for engineering and technological applications, the Young's modulus and the Poisson's ratio are 223.8 and 0.28, respectively. The first one, which provides a measure of the stiffness of the YGG, has a high value hence the YGG is a hard material, and the second one is close to 0.3, thus suggesting that YGG is a material with predominant central internal forces. Note that the overall high coordination of the atoms tends to bring the system to a quasispherical symmetry causing the central forces to dominate the mechanical properties.

C. Electronic structure

The electronic structure of a material is related with the optical and transport properties and plays a major role in the reactivity and stability of the material. The calculated direct band gap of 3.51 eV is located at the Γ point at ambient

Downloaded 09 May 2013 to 158.42.242.92. This article is copyrighted as indicated in the abstract. Reuse of AIP content is subject to the terms at: http://jap.aip.org/about/rights_and_permissions

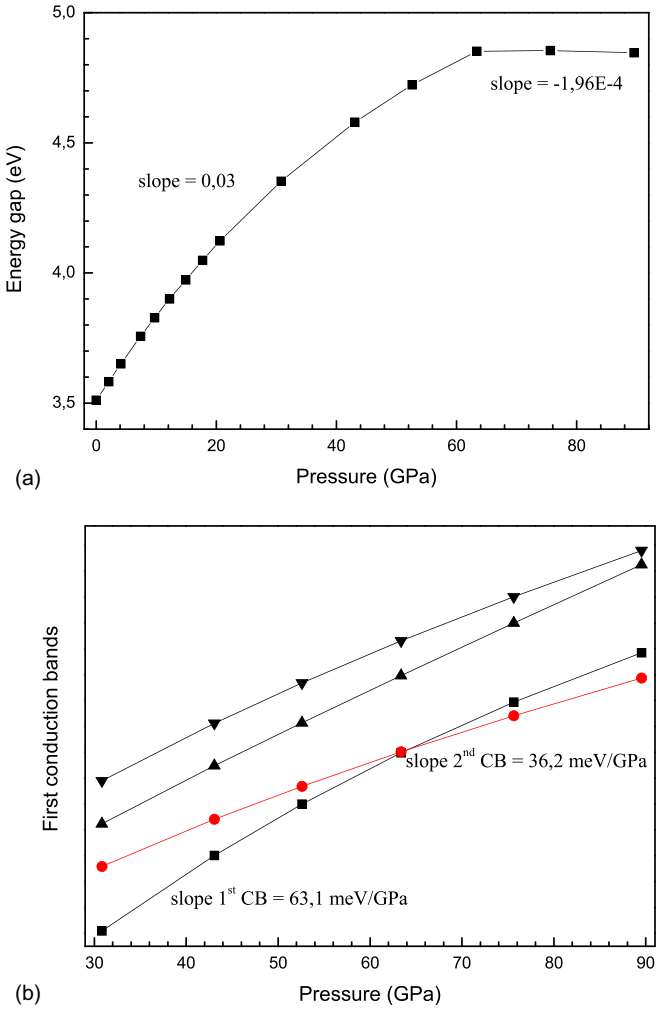

FIG. 6. (a) The pressure dependence of direct gap at Γ point and (b) representation of first four conduction bands vs. Pressure at Γ point. At 63.38 GPa, the intersection of first and second CB is showed.

pressure. It is well known that DFT calculations underestimate the band gap, but they provide a good description of the pressure dependence of the band gap. Figure 6(a) shows the pressure dependence of the direct band gap at the Γ point in YGG. It can be observed that the direct band gap increases at a rate of 30 meV/GPa at low pressures, but it decreases above 63 GPa. This behaviour of the direct band gap can be understood by observing the pressure dependence of the conduction bands, CBs, at the Γ point plotted in Fig. 6(b). It can be observed that the first conduction band, CB, has a pressure coefficient of 63.1 meV/GPa and crosses the second CB, with a pressure coefficient of 36.2 meV/GPa, at 63 GPa. Therefore, the first (second) CB becomes the second (first) CB above 63 GPa. The direct band gap shows a negative pressure coefficient above 63 GPa.

In order to understand the pressure-induced band gap crossing at the Γ point, we have plotted in Figs. 7(a) and 7(b) the theoretical electronic band structure of YGG at 0 and 75.6 GPa, respectively. It can be observed that the top of the valence band (VB) is very flat and similar to other garnets[7,23,24] or Y- and Al-related compounds. On the other hand, the conduction band (CB) edge at Γ point consists of a rather well-separated band with respect to other CBs. As the first CB (red in Fig. 7) shows a strong positive pressure coefficient with increasing pressure it crosses the second CB (blue in Fig. 7), with a much smaller pressure coefficient, above 63 GPa.

In order to better explain the different behaviour between the first and second CBs with pressure we have plotted in Figs. 8(a) and 8(b) the total density of states (DOS) and the atom-resolved partial density of states (PDOS) of YGG garnet at 0 and 75.6 GPa, respectively. From the PDOS, we are able to identify the angular momentum characters of different structures in the DOS. In the VB, the O-2 s levels mainly contribute at −16 eV at 0 GPa and −18 eV at 75.6 GPa, with small contributions in the upper VB and at the bottom of CB. The O-2 p levels are mainly in the upper valence band with a width of almost 8 eV and in the CB with a width of 5 eV. On the other side, Ga_{tet}-4 s and Ga_{tet}-4 p levels are situated in the VB with an important contribution in the top of VB, while they have a smaller contribution in the CB. The Ga_{tet}-3 d orbitals have energy of −12 eV and also contribute in the upper VB and at the bottom of CB. The only effect of the pressure on the Ga_{tet} orbitals is a little displacement in their energies. A similar situation holds for Ga_{oct} orbitals. The only difference with respect to Ga_{tet} is that there is not contribution of Ga_{oct}-3 d levels in the CB. Finally, concerning Y orbitals, Y-4 s levels have a very low energy (−38 eV at 0 GPa and −40 eV at 75.6 GPa). These levels are semicore of Y atoms but in this study are treated as valence states similar to Y-4 p levels. Another s orbital of Y (Y−5 s) is projected in higher VB and Y-4 p orbital is

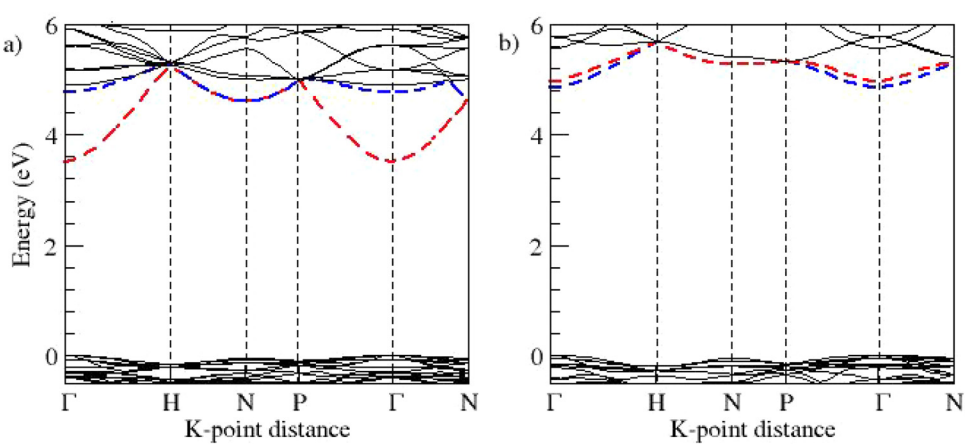

FIG. 7. The band structure of the YGG (a) at 0 GPa and (b) at 75 GPa. The red dashed line is the first conduction band and the blue dashed line is the second conduction band.

Downloaded 09 May 2013 to 158.42.242.92. This article is copyrighted as indicated in the abstract. Reuse of AIP content is subject to the terms at: http://jap.aip.org/about/rights_and_permissions

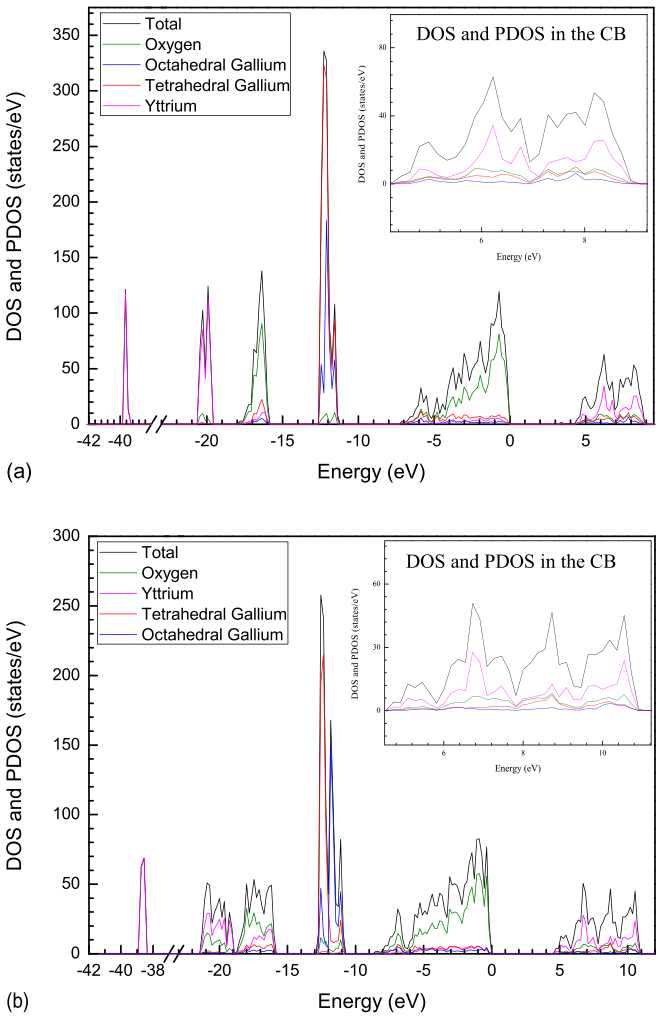

FIG. 8. (a) The calculated total DOS and atom-resolved PDOS of YGG at 0 GPa and (b) at 75 GPa. The total DOS is the black curve. The PDOS of Y atoms is the pink curve and that of Ga_{oct} and Ga_{tet} atoms correspond to the blue and red curve, respectively, and the PDOS of O atoms is the green curve.

around −20 eV at 0 GPa and −21 eV at 75.6 GPa with contributions in the upper VB and CB. Y-4 d orbital plays an important role in the CB; while the pressure increases, the Y-4 d projected wave function character of the conduction bands increases. It is worth noting the enhancement of its contribution in the first CBs. Consequently, this increase of Y-4 d orbitals could cause hybridization changes because of the presence of the Ga_{tet} and Ga_{oct} orbitals and O−2 s (2 p) orbitals. The pressure dependence of the energy band of the YGG is compared with that of the YAG. The band gap energy of YAG decreases and the band structure is the same as the pressure increases.[7,24] The only difference between the YAG and YGG is the presence of gallium atoms in the structure. For this reason, the valence orbitals of gallium (Ga) atoms and of Y atoms could affect to the electronic behaviour of YGG because of hybridization change. Concretely, the contribution of the s and p orbitals of octahedral gallium, tetrahedral gallium and yttrium increase in the upper VB with an enhancement of their widths of 1.5 eV in gallium ions and from 4 to 7 eV in yttrium ions at 75 GPa. On the other side, in the conduction bands, there are not variation of the s and p orbitals of the two kinds of gallium and yttrium. The important difference in the CBs is the variation of the Ga_{tet}-3 d and Y-4 d orbitals, increasing their widths from 4 to 6 eV and from 5 to 7 eV, respectively, and the increase of the contribution of the Y-4 d levels in the first conduction bands.

IV. CONCLUSIONS

We have performed a theoretical study of the structural, elastic, and electronic properties of yttrium gallium garnet, $Y_3Ga_5O_{12}$, under hydrostatic pressure. The calculated structural ground state properties are in good agreement with the available experimental data. Pressure dependence of the elastic constants and the mechanical stability are analysed up to 90 GPa, showing that the garnet is mechanically unstable above 84 GPa. We also present the electronic band structure calculations which show upon compression the fundamental direct gap and an exchange between the first and second CB. The direct gap increases up to 63 GPa and later monotonically decreases under pressure.

ACKNOWLEDGMENTS

This work has been supported by Ministerio de Ciencia e Innovación of Spain (MICINN) under the National Program of Materials (MAT2010-21270-C04-02/03/04) and the Consolider-Ingenio 2010 Program (MALTA CSD2007-0045), by the Vicerrectorado de Investigación y Desarrollo of the Universitat Politècnica de València (UPV2011-0914 PAID-05-11 and UPV2011-0966 PAID-06-11) and by the EU-FEDER funds. V. Monteseguro wishes to thank MICINN for the FPI Grant (BES-2011-044596). We thank the computer time provided by the Red Española de Supercomputación (RES).

[1]A. Speghini, F. Piccinelli, and M. Betinelli, Opt. Mater. **33**, 247–257 (2011).
[2]F. Wang and X. Liu, Chem. Soc. Rev. **38**, 976–989 (2009).
[3]D. Hreniak, W. Strek, P. Gluchowski, M. Bettinelli, and A. Speghini, Appl. Phys. B **91**, 89–93 (2008).
[4]E. Caponetti, D. C. Martino, M. L. Saladino, and C. Leonelli, Langmuir **23**, 3947–3952 (2007).
[5]R. Krsmanovic, V. A. Morozov, O. I. Lebedev, S. Polizzi, A. Speghini, M. Bettinelli, and G. Van Tendeloo, Nanotechnology **18**, 325604–325612 (2007).
[6]R. Naccache, F. Vetrone, A. Speghini, M. Bettinelli, and J. A. Capobianco, J. Phys. Chem. C **112**, 7750–7756 (2008).
[7]Y.-N. Xu and W. Y. Ching, Phys. Rev. B **59**, 10530 (1999).
[8]P. Goel, R. Mittal, N. Choudhury, and S. L. Chaplot, J. Phys. Condens. Matter **22**, 065401 (2010).
[9]A. Mujica, A. Rubio, A. Muñoz, and R. J. Needs, Rev. Mod. Phys. **75**, 863 (2003).
[10]P. Hohenberg and W. Kohn, Phys. Rev. **136**, B864 (1964).
[11]G. Kresse and J. Hafner, Phys. Rev. B **47**, 558 (1993); **49**, 14251 (1994); G. Kresse and J. Furthmüller, Comput. Mater. Sci. **6**, 15 (1996); Phys. Rev. B **54**, 11169 (1996).
[12]P. E. Blöchl, Phys. Rev. B **50**, 17953 (1994); G. Kresse and D. Joubert, *ibid.* **59**, 1758 (1999).
[13]J. P. Perdew, A. Ruzsinszky, G. I. Csonka, O. Vydrow, G. E. Scuseria, L. A. Constantin, X. Zhou, and K. Burke, Phys. Rev. Lett. **100**, 136406 (2008).

Downloaded 09 May 2013 to 158.42.242.92. This article is copyrighted as indicated in the abstract. Reuse of AIP content is subject to the terms at: http://jap.aip.org/about/rights_and_permissions

[14]N. Chetty, A. Muñoz, and R. M. Martin, Phys. Rev. B **40**, 11934–11936 (1989).
[15]S. Baroni, S. de Gironcoli, A. Dal Corso, and P. Giannozzi, Rev. Mod. Phys. **73**, 515–562 (2001).
[16]O. Beckstein, J. E. Klepeis, G. L. W. Hart, and O. Pankratov, Phys. Rev. B **63**, 134112 (2001).
[17]J. F. Nye, *Physical Properties of Crystals. Their Representation by Tensor and Matrices* (Oxford University Press, 1957).
[18]M. Born and H. Kun, *Dynamical Theory of Crystal Lattices* (Oxford University Press, 1954).
[19]J. Wang and S. Yip, Phys. Rev. Lett. **71**, 4182 (1993).
[20]A. Nakatsuka, A. Yoshiasa, and S. Takeno, Acta Crystallogr. **51**, 737–745 (1995).
[21]F. Birch, Phys. Rev. **71**, 809 (1947).
[22]V. Milman, R. H. Nobes, E. V. Akhmatskaya, B. Winkler, C. J. Pickard, and J. A. White, *Ab Initio* Study of the Structure and Compressibility of Garnets, In Properties of Complex Inorganic Solids 2, edited by A. Meike, A. Gonis, P. E. A. Turchi, and K. Rajan (Kluwer Academic/Plenum, New York, 2000), pp. 417–427.
[23]V. Monteseguro *et al*. private communication (2013).
[24]V. Monteseguro *et al*. (unpublished).
[25]E. Husson, C. Proust, P. Guillet, and J. P. Itie, Mater. Res. Bull. **34**, 2085 (1999).
[26]H. Wang, Y. He, Y. W. Zeng, K. Stahl, T. Kihegawa, and J. Z. Jiang, J. Appl. Phys. **107**, 033520 (2010).
[27]F. Euler and J. A. Bruce, Acta Crystallogr. **19**, 971 (1965).
[28]K. Papagelis, J. Arvanitidis, E. Vinga, D. Christofilos, G. A. Kourouklis, H. Kimura, and S. Ves, J. Appl. Phys. **107**, 113504 (2010).
[29]B. B. Karki, G. J. Ackland, and J. Crain, J. Phys. Condens. Matter. **9**, 8579 (1997).
[30]G. A. Saunders, S. C. Parker, N. Benbattouche, and H. I. Alberts, Phys. Rev. B **46**, 8756 (1992).
[31]Y. K. Yogurtcu, A. J. Miller, and G. A. Saunders, J. Phys. C **13**, 6585 (1980).
[32]H. Hua, S. Mirov, and Y. K. Vohra, Phys. Rev. B **54**, 6200 (1996).

Downloaded 09 May 2013 to 158.42.242.92. This article is copyrighted as indicated in the abstract. Reuse of AIP content is subject to the terms at: http://jap.aip.org/about/rights_and_permissions